

Contemporary presence of dynamical and statistical production of intermediate mass fragments in midperipheral $^{58}\text{Ni}+^{58}\text{Ni}$ collisions at 30 MeV/nucleon

P.M.Milazzo ^a, G.Vannini ^b, M.Sisto ^a, C.Agodi ^c, R.Alba ^c,
 G.Bellia ^c, M.Belkacem ^d, M.Bruno ^b, M.Colonna ^c, N.Colonna ^e,
 R.Coniglione ^c, M.D'Agostino ^b, A.Del Zoppo ^c, L.Fabietti ^f,
 P.Finocchiaro ^c, F.Gramegna ^g, I.Iori ^f, K.Loukachine ^c,
 C.Maiolino ^c, G.V.Margagliotti ^a, P.F.Mastinu ^g, E.Migneco ^c,
 A.Moroni ^f, P.Piattelli ^c, R.Rui ^a, D.Santonocito ^c, P.Sapienza ^c,
 P.Ventura ^c

^a*Dipartimento di Fisica and INFN, Trieste, Italy*

^b*Dipartimento di Fisica and INFN, Bologna, Italy*

^c*INFN, Laboratori Nazionali del Sud, Catania, Italy*

^d*University of Minnesota, USA*

^e*INFN, Bari, Italy*

^f*Dipartimento di Fisica and INFN, Milano, Italy*

^g*INFN, Laboratori Nazionali di Legnaro, Italy*

Abstract

The $^{58}\text{Ni} + ^{58}\text{Ni}$ reaction at 30 MeV/nucleon has been experimentally investigated at the Superconducting Cyclotron of the INFN Laboratori Nazionali del Sud. In midperipheral collisions the production of massive fragments ($4 \leq Z \leq 12$), consistent with the statistical fragmentation of the projectile-like residue and the dynamical formation of a neck, joining projectile-like and target-like residues, has been observed. The fragments coming from these different processes differ both in charge distribution and isotopic composition. In particular it is shown that these mechanisms leading to fragment production act contemporarily inside the same event.

Key words: Heavy Ions, Multifragmentation

PACS: 25.70.Pq, 25.70.-z

The production of intermediate mass fragments (IMF, $3 \leq Z \leq 20$) is the distinguishing feature of intermediate energy heavy ion collisions. A possible scenario for IMF emission involves the development of bulk instabilities in the nuclear matter, which lead to a statistical fragmentation. This is supported by several experimental results concerning both the decay of

unique sources formed in central collisions and the disassembly of quasitarget (QT) and quasiprojectile (QP) in dissipative peripheral collisions [1,2].

On the other hand theoretical studies of the collision dynamics predict the formation of highly deformed nuclei in this energy regime [3] and experimental evidences have been collected on the role of the formation and decay of neck-like structures in IMF production [4,5]. Nevertheless it is still unclear when this reaction mechanism sets in. For medium mass systems Boltzmann-Nordheim-Vlasov (BNV) calculations predict the onset of neck instabilities to occur for energies between 30 and 70 MeV/nucleon [3]. For lower energies the interaction time between the projectile and the target is sufficiently long for the neck to be reabsorbed by the QP and/or the QT, whereas for higher energies the system evolves towards a fireball regime.

The study of the formation and decay of neck-like structures has a variety of theoretical implications. The beam energy at which a neck zone is formed and decays depends on the Equation of State (EOS) of the nuclear matter [6]; a soft EOS favours neck formation (because of a smaller orbiting) and rupture. Similarly an isospin dependence of the EOS is also expected to influence the process of formation and decay of an intermediate source and this should reflect on the neutron-to-proton ratio of the emitted fragments [7].

The present analysis of the Ni+Ni midperipheral collisions is aimed to investigate the interplay, inside the same event, between dynamically driven neck instabilities and QP statistical fragmentation in IMF production.

The experiment was performed at the INFN Laboratori Nazionali del Sud with MEDEA [8] and MULTICS [9] apparatus. A beam of ^{58}Ni at 30 MeV/nucleon bombarded a 2 mg/cm² thick nickel target. The angular range $3^\circ < \theta_{lab} < 28^\circ$ was covered by the MULTICS array [9], consisting of 55 telescopes, each of which was composed of an Ionization Chamber (IC), a Silicon detector (Si) and a CsI crystal. Typical energy resolutions were 2%, 1% and 5% for IC, Si and CsI, respectively. The threshold for charge identification in the MULTICS array was about 1.5 MeV/nucleon. A good mass resolution for Z=1-6 isotopes was obtained above 8.5, 10.5, 14 MeV/nucleon for ^4He , ^6Li and ^{12}C nuclei, respectively [2]. Light charged particles (Z=1,2) and γ -rays were detected at $30^\circ < \theta_{lab} < 170^\circ$ by the BaF₂ ball of the MEDEA apparatus. The geometric acceptance of the combined array was greater than 90% of 4π .

Since the relatively small number of detected fragments and particles ($N_c \leq 5-6$) makes not possible an accurate impact parameter selection, using the standard methods [10], we followed a different approach: 1) selecting only the "complete" multifragment events, i.e. events where at least three IMF were produced and at least 80% of the total linear momentum was detected; 2) defining peripheral and midperipheral collisions those for which the heaviest fragment (with charge at least 1/3 of that of the projectile, i.e. $Z \geq 9$) travels, in the laboratory frame, with a velocity higher than 80% of that of the projectile ($v_P = 7.6$ cm/ns). Accordingly, since the energy thresholds make not possible the detection of the QT reaction products, we find that the total detected charge (Z_{TOT}) does not differ from that of the projectile for more than 30% ($20 \leq Z_{TOT} \leq 36$). Considering that not completely detected central events can simulate complete non-central ones, we checked the existence in central events of heavy fragments ($Z \geq 9$) moving faster than 5.6 cm/ns, i.e. compatible with the QP velocity. Central collision events have been selected requiring that the heaviest fragment has a velocity close to the center of mass one and that the total detected charge is at least

80% of the initial (projectile + target) value. We found that such a kind of contamination is completely absent.

To get information about the impact parameters range selected by this procedure and by the apparatus acceptance, the experimental data have been compared with the predictions of classical molecular dynamics (CMD) calculations [11]. CMD events are plotted in Fig.1a; the dot-filled area refers to the amount of "complete" multifragmentation events (with at least three IMF products) after experimental efficiency filtering. In the dark area of Fig.1a we present the filtered complete events with the further condition that the heaviest fragment moves with a velocity higher than the 80% of v_P . It becomes evident how midperipheral impact parameter are preferentially selected.

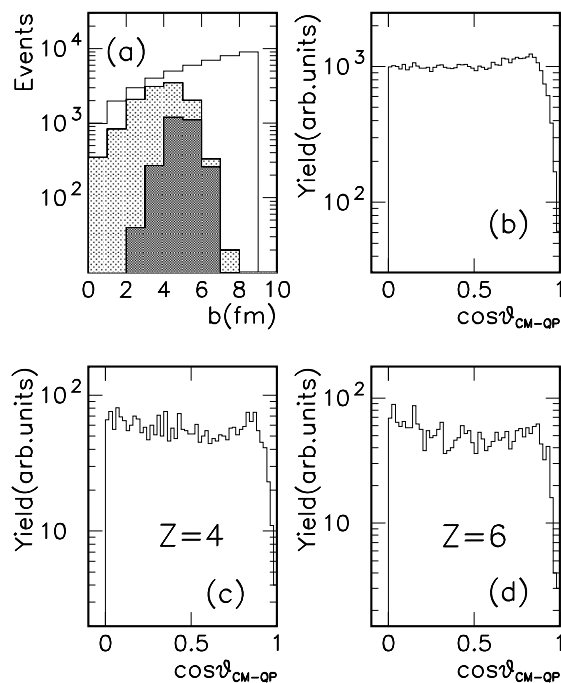


Fig. 1. (a) Yields from CMD calculations: raw data (blank area), multifragmentation events after apparatus efficiency (dot-filled area), with further constraints on the heaviest fragments (dark area), (b-d) Angular distributions for IMF forward emitted by the quasiprojectile (all charged particle (b), $Z=4$ (c) and $Z=6$ (d) fragments).

The results presented hereafter will refer only to midperipheral events with at least three IMF, with the aim of observing the IMF emitting sources. To this respect we present in Fig.2 the distributions of the parallel component of the velocity, with respect to the beam direction, for different Z values. For carbon and oxygen nuclei two distinct distributions are evident: the first is centered at 6.5 cm/ns (the QP velocity) and the second one is at the center of mass velocity (3.8 cm/ns), intermediate between that of the target and of the projectile, because of the system symmetry. Fig.2b-c show, in events where both the heaviest fragment and an oxygen nucleus have velocities close to that of the projectile, the yield of a third fragment (dot-dashed lines). It appears that this latter fragment has a great probability of being emitted with a velocity centered around that of the c.m.. This is evidence that, while the QP is decaying in two or more fragments, there is another system emitting

IMF, intermediate (IS) between the QP and QT.

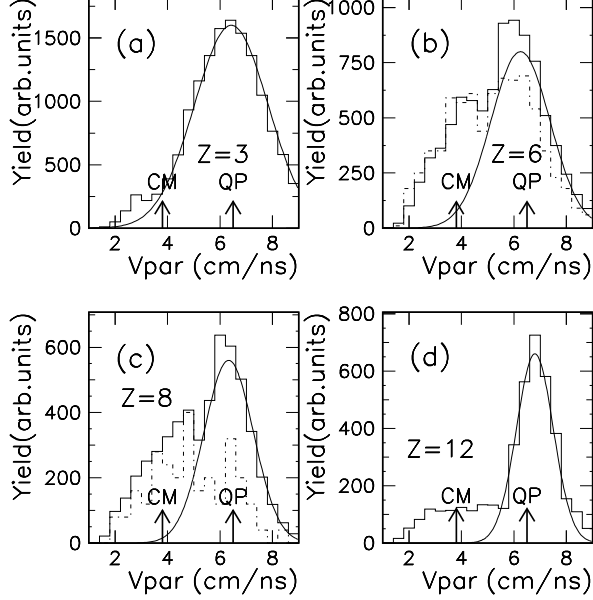


Fig. 2. v_{par} distributions for $Z=3, 6$ (dot-dashed line, multiplied by a factor 10), 8 (dot-dashed line, multiplied by a factor 40), 12 ; the arrows refer to the center of mass (CM) and QP velocities.

With the same event selection used for the fragment analysis for midperipheral collisions we considered the proton spectra detected by the MEDEA apparatus. Eight energy spectra, measured at different laboratory angles, were simultaneously fitted by the superposition of three Maxwellian distribution. The fit results put in evidence the existence of a fast source (6.8 cm/ns and slope parameter $T_{slope} \simeq 5.1$ MeV) consistent with the QP, an almost at rest source (QT system, 0.8 cm/ns, $T_{slope} \simeq 4.3$ MeV) and an intermediate velocity source (3.8 cm/ns) with high slope parameter ($T_{slope} \simeq 10.1$ MeV). Moreover the QP and QT source show the same proton multiplicity. The intermediate velocity component has been generally interpreted as also due to pre-equilibrium emission in the interacting zone [12]. These results are compatible with those shown in Ref.[13].

These results show that in midperipheral collisions three different emitting sources are present; there are events in which the IMF can be simultaneously produced by the decay of QP and QT (its fragments are not seen because under energy threshold for identification) sources and from a neck, forming a midvelocity emission source. Thus, disentangling the contributions from the QP and the neck sources becomes a mandatory requirement to improve the understanding of the IMF production mechanism and perform comparisons of the IMF experimental yields with theoretical predictions. To this purpose we first study the process leading to the disassembly of the QP restricting the analysis to the fragments emitted with $v_{par} > 6.5$ cm/ns (see Fig.2). This constraint allows the selection of the decay products forward emitted in the QP decay with negligible contamination due to QT and midrapidity source emissions. To check if the QP reaches an equilibration stage before its de-excitation we studied in its reference frame the angular and energy distributions of the emitted fragments. Angular distributions are presented in Figg.1b-d; they are flat and then in agreement with the hypothesis of an isotropic emission; this is a necessary condition to

establish a possible equilibration of the studied system. On the other hand fitting the energy distributions of different isotopes with Maxwellian functions we get, for all the detected isotopes ($3 \leq A \leq 14$), similar values (within errors) for the apparent temperatures T_{slope} . This behaviour gives indications that the condition of equilibration of the fragmenting systems is satisfied. In Figg.3a-e the energy distributions of different isotopes are presented. Each panel (from a to d) refers to two different isotopes of the same element to put in evidence the similarity of shapes and slopes; in the (e) panel the Maxwellian fit is superimposed to the experimental data showing the accuracy of the obtained results.

To gain more insight in the equilibration of the QP we compared the experimental charge distribution with the microcanonical Statistical Multifragmentation Model (SMM) predictions [15], performed for a Ni nucleus at one third of the normal density. The events generated by SMM at different input excitation energies were filtered by the experimental acceptance. The experimental charge distribution is quite well reproduced assuming an excitation energy of 4 MeV/nucleon (Fig.3f).

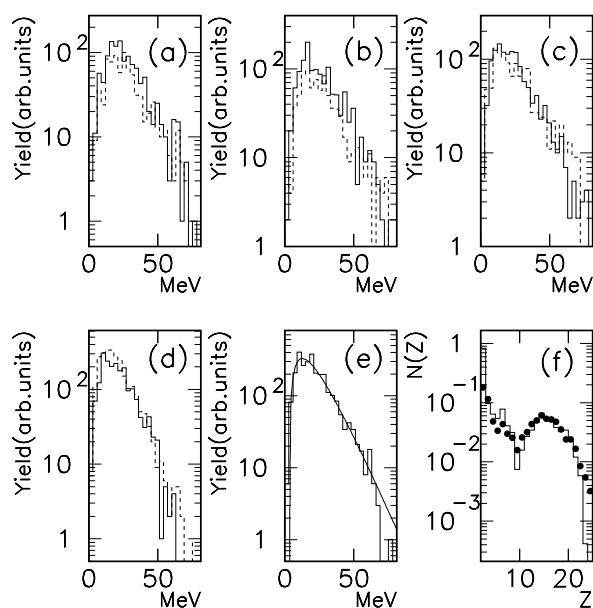


Fig. 3. (a-e) Energy distributions for different isotopes (a - ^{12}C (full line), ^{13}C (dashed line), b - ^{10}B (full), ^{11}B (dashed), c - ^7Be (full), ^9Be (dashed), d - ^6Li (full), ^8Li (dashed), e - Maxwellian fit for ^7Li , $T_{slope}=8.9$ MeV); (f) mean elemental event multiplicity $N(Z)$ for QP fragments (solid point: experimental data, histogram: SMM predictions).

The evidences of the equilibration of the QP source allow investigating some characteristics, such as the temperature and the excitation energy. We extract the temperature T through the method of double ratios of isotope yields [16]. As this method requires that the nuclei originate from the same emitting source, only the $Z \geq 3$ fragments forward emitted ($v_{par} \geq 6.5$ cm/ns, velocity of the QP in the laboratory frame) were considered. Table 1 gives the values for the most reliable thermometers [16,17]. Since experimental temperature measurements are affected by secondary decays, we also report in Table 1 the values corrected as suggested in Ref.[17]. Their mean value, $T_0=3.9 \pm 0.3$ MeV, can be considered as the break-up temperature of the QP decaying system.

Table 1

Table 1

Temperatures of the QP system extracted from different double yield isotope ratio (T_{exp}) and calculated values after sequential feeding correction (T_{corr}).

	T_{exp} (MeV)	T_{corr} (MeV)
${}^6Li/{}^7Li - {}^{11}C/{}^{12}C$	3.9 ± 0.2	3.3 ± 0.3
${}^9Be/{}^{10}Be - {}^{11}C/{}^{12}C$	6.7 ± 0.9	3.7 ± 0.5
${}^{10}B/{}^{11}B - {}^{11}B/{}^{12}B$	4.3 ± 0.5	4.3 ± 0.5
${}^{11}B/{}^{12}B - {}^{11}C/{}^{12}C$	4.3 ± 0.3	4.4 ± 0.3
${}^{11}C/{}^{12}C - {}^{12}C/{}^{13}C$	3.7 ± 0.2	3.6 ± 0.2

Besides the indication given by the statistical model, we can give a rough estimate of the upper limit of the excitation energy using the energy conservation and assuming that on average there is an equal sharing of excitation energy between QP and QT. Then in the center of mass frame we have: $E_{QP}^* = \frac{1}{2}(m_P v_P^2 - m_{QP} v_{QP}^2) + E_{NECK}^*$, where m_P , m_{QP} , v_P , v_{QP} are mass and velocity of projectile and QP, respectively. Neglecting the amount of energy transferred to the neck source (admittedly small to avoid its complete vaporization) and taking into account the mass difference between the projectile and the QP, the maximum of excitation energy ranges from 3.7 (if no nucleon transfer to a neck is assumed) up to 5.9 MeV/nucleon (half nickel is lost in the reaction); if, for instance, we require the formation of an oxygen nucleus in the center of mass source we have accordingly an estimate of $\simeq 4.5$ MeV/nucleon. This rough estimation completely neglects other dissipation processes, as pre-equilibrium emission.

The temperature and excitation energy values extracted in the present case are quite similar to those measured [2] for the QP fragmentation in the ${}^{197}Au + {}^{197}Au$ reaction at 35 MeV/nucleon ($T_0=3.9\pm 0.2$ MeV, an upper limit of the excitation energy $\simeq 4.5$ MeV/nucleon and a corresponding measured (and also predicted by SMM) value of $\simeq 4$ MeV/nucleon). In Ref.[2] it has been found good agreement between the excitation energy values obtained following different methods (calorimetric [18], comparison with SMM predictions, rough estimation of the upper limit), in the range (3-6 MeV/nucleon).

In conclusion the present data analysis shows that the QP source has attained thermal equilibrium and that fragmentation is its main de-excitation process, well reproduced by a statistical approach.

As already shown, in coincidence with the statistical fragmentation of the QP, we observed the emission of IMF from a IS. In the following we will discuss in detail the properties of this IMF emission at midrapidity. The expected distribution of the fragment velocity v_{par} from the multifragmentation of the QP source is Gaussian. Thus the QP region of the v_{par} distribution has been fitted, for each fragment Z value, with a Gaussian function, giving the experimental QP yield (Y_{QP}). The fit parameters were extracted taking into account only the $v_{par} \geq 6.5$ cm/ns part. In Fig. 2 the results are plotted, together with the experimental yields. Similar behaviors have been found for all atomic numbers in the range $3 \leq Z \leq 14$. Due to the experimental energy threshold (for the QT source side) the presented spectra are not symmetric around the c.m. velocity. To avoid possible contamination in the midrapidity region we evaluated the yield (Y_{NECK}) from the IS source as twice the difference between the whole v_{par} distribution for velocities higher than that of the c.m. and Y_{QP} . This was

done to avoid distortions due to efficiency effects and possible QT contaminations for the lowest velocities. We checked that in the considered Z range the experimental inefficiency doesn't affect the above-mentioned procedure [9].

In Fig.4a the ratio between the relative yields (Y_{NECK}/Y_{QP}) is presented as a function of the atomic number Z . We observe a bell-like shape, peaked around $Z=9$. We notice the high probability of IMF emission from the neck zone when the event IMF multiplicity is at least 3 [4]. The presence of this maximum could be an effect of the breakup geometry; in fact, a rough consistency has been found with percolative calculations that compare emissions from a cylindrical shape neck, joining spherical QT and QP, and from the QP itself [5,14]. If on one side the QP disassembly is ruled by statistical models after thermal equilibrium has been reached, on the other side the neck emission exhibit quite different features that cannot be reproduced making statistical equilibrium assumptions. We have thus performed BNV calculations using different EOS parameters [3]. We found that with a compressibility term K of 200 MeV (soft EOS) there is an evident massive neck formation (after 200 fm/c), that is not reabsorbed by the QP or the QT (this behaviour disappears increasing the K values). These calculations predict that on average we have a $Z=8$ fragment in the neck zone, and show that the IS fragment production comes from material which is "surface-like" (since it originates from the overlap of the surfaces of the two nuclei) and which could be neutron rich [7]. To investigate the neutron content of the neck matter we observed the ${}^6\text{He}$ experimental yield. Its emission is quasi negligible from a statistical decay, both because the binding energy favours, for $Z=2$, α particle emission and because the N/Z value of ${}^6\text{He}$ is quite different from the corresponding ratio of the system ($N/Z=2$ for ${}^6\text{He}$, $N/Z=30/28 \simeq 1$ for the system). If the surfaces of the interacting nuclei are more neutron rich than the bulk matter or the dynamical process leading to the formation of a neck structure has a particular isospin dependence, the ${}^6\text{He}$ production should be more abundant in the neck zone with respect to the QP zone. In Fig. 4b the experimental ${}^4\text{He}$ and ${}^6\text{He}$ yields are plotted versus v_{par} : one can see that, while the ${}^4\text{He}$ distribution is centered around the QP velocity (with a small emission from the neck zone) the ${}^6\text{He}$ yield is very scarce in the QP zone and starts to increase going towards the midvelocity region. One should take into account that the energy thresholds for mass identification are greater than for Z identification and that in the He case they produce cuts for velocities lower than 4 cm/ns. To better see the isospin effect in Fig.4c-d the $Y({}^6\text{He})/Y({}^4\text{He})$ and $Y({}^3\text{He})/Y({}^4\text{He})$ yield ratios are plotted. The amount of more rich (poor) neutron He -isotopes increases (decreases) going towards the midvelocity region. The behaviour of these ratios clearly shows the increase of neutron content in the midvelocity zone with respect to the interacting matter. This is a further indication that in midperipheral collisions we observe an IMF production which is due to two different mechanisms: one of statistical and the other of dynamical nature.

In conclusion, in the study of the Ni+Ni 30 MeV/nucleon dissipative midperipheral collisions it has been possible to reveal events in which the IMF's are emitted by two different sources with different mechanisms. We are in presence of a QP (and a QT), with an excitation energy which leads to the multifragmentation regime; its decay can be fully explained in terms of a statistical disassembly of a thermalized system ($T=3.9 \pm 0.2$ MeV, $E^* \simeq 4$ MeV/nucleon). Contemporary to the IMF production from the QP source an intermediate source is formed, emitting both light particles and IMF. These fragments are more neutron rich than the average matter of the overall system and have a quite different charge distribution, with respect to the ones statistically emitted from the QP. These features can be considered as a signature of the dynamical origin of the midvelocity emission. The presented results then

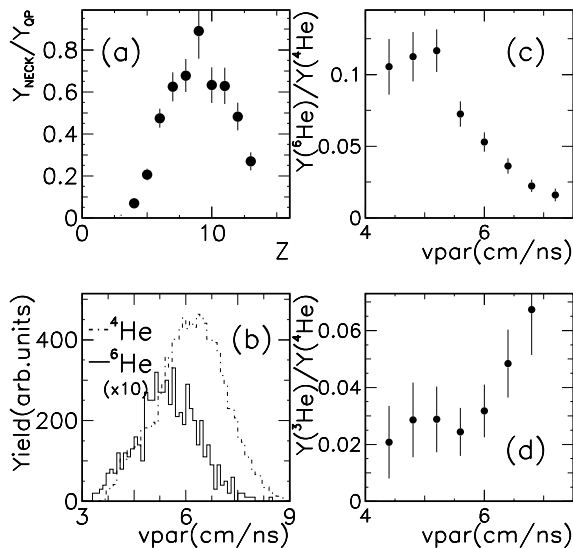


Fig. 4. (a) Ratio of the measured yields for neck fragmentation and QP emission; (b) Yields of ${}^4\text{He}$ (dot-dashed line) and ${}^6\text{He}$ (full line, multiplied by a factor 10); $Y({}^6\text{He})/Y({}^4\text{He})$ (c) and $Y({}^3\text{He})/Y({}^4\text{He})$ (d) yield ratios as a function of v_{par} .

show that IMF can be produced via different mechanisms that can find contemporary room inside the same collision.

References

- [1] J. Pochodzalla *et al.*, Phys. Rev. Lett., **75** 1040 (1995); J. B. Elliot *et al.*, Phys. Rev. C **49**, 3185 (1994); M. L. Gilkes *et al.*, Phys. Rev. Lett., **73**, 1590 (1994); J. A. Hauger *et al.*, Phys. Rev. C **57**, 764 (1998); P. F. Mastinu *et al.*, Phys. Rev. Lett., **76**, 2646 (1996); M. D'Agostino *et al.*, Nucl. Phys. **A650**, 329 (1999).
- [2] P. M. Milazzo *et al.*, Phys. Rev. C **58**, 953 (1998).
- [3] W. Bauer *et al.*, Phys. Rev. Lett., **69**, 1888 (1992); M. Colonna *et al.*, Nucl. Phys., **A583**, 525 (1995); M. Colonna *et al.*, Nucl. Phys., **A589**, 2671 (1995).
- [4] G. Casini *et al.*, Phys. Rev. Lett., **71**, 2567 (1993); J. Toke *et al.*, Phys. Rev. Lett., **75**, 2920 (1995); Y. Larochelle *et al.*, Phys. Rev. C **55**, 1869 (1997); J. Lukasik *et al.*, Phys. Rev. C **55**, 1906 (1997); P. Pawlowski *et al.*, Phys. Rev. C **57**, 1711 (1998).
- [5] C. P. Montoya *et al.*, Phys. Rev. Lett., **73**, 3070 (1994).
- [6] L. G. Sobotka *et al.*, Phys. Rev. C **50**, R1272 (1994).
- [7] J. F. Dempsey *et al.*, Phys. Rev. C **54**, 1710 (1996).
- [8] E. Migneco *et al.*, Nucl. Instr. and Meth. Phys. Res., **A314** 31 (1992).
- [9] I. Iori *et al.*, Nucl. Instr. and Meth. Phys. Res., **A325** 458 (1993).

- [10] C. Cavata *et al.*, Phys. Rev. C **42**, 1760 (1990).
- [11] M. Belkacem *et al.*, Phys. Rev. C **52**, 271 (1995).
- [12] R. Alba *et al.*, Phys. Lett. B **322**, 38 (1994); P. Sapienza *et al.*, Phys. Rev. Lett., **73**, 1769 (1994); R. Coniglione *et al.*, to appear in Phys. Lett. B .
- [13] E. Ramakrishnan, *et al.*, Phys. Rev. C **57**, 1803 (1998).
- [14] W. Bauer *et al.*, Nucl. Phys., **A452**, 699 (1986); W. Bauer *et al.*, Phys. Rev. C **38**, 1927 (1988).
- [15] J.P. Bondorf *et al.*, Nucl. Phys. **A444** (1986) 460; A. S. Botvina *et al.*, Nucl. Phys. **A475** (1987) 663; J.P. Bondorf *et al.*, Phys. Rep. **257** (1995) 133.
- [16] S. Albergo *et al.*, Nuovo Cimento **89**, 1 (1985).
- [17] M. B. Tsang *et al.*, Phys. Rev. Lett., **78**, 3836 (1997); H.Xi *et al.*, Phys. Lett. **B431** 8 (1998).
- [18] X.Campi *et al.*, Phys. Rev. C **50**, (1994) R2680.